

Spectroscopic evidence for strong correlations between local resistance and superconducting gap in ultrathin NbN films

C. Carbilliet¹, V. Cherkez¹, M.A. Skvortsov^{2,3}, M.V. Feigel'man^{3,2}, F. Debontridder¹, L.B. Ioffe^{4,3}, V.S. Stolyarov^{1,5,6}, K. Ilin⁷, M. Siegel⁷, D. Roditchev^{1,8}, T. Cren¹, and C. Brun^{1*}

¹*Sorbonne Université, CNRS, Institut des Nanosciences de Paris, UMR7588, F-75252, Paris, France*

²*Skolkovo Institute of Science and Technology, Moscow 121205, Russia*

³*L. D. Landau Institute for Theoretical Physics, Chernogolovka 142432, Russia*

⁴*Sorbonne Université, CNRS, LPTHE, UMR 7589, F-75252, Paris, France*

⁵*Moscow Institute of Physics and Technology, 141700 Dolgoprudny, Russia*

⁶*Institute of Solid State Physics RAS, 142432 Chernogolovka, Russia*

⁷*Institute of Micro- und Nano-electronic Systems, Karlsruhe Institute of Technology, Hertzstrasse 16, D-76187 Karlsruhe, Germany and*

⁷*LPEM, ESPCI Paris-PSL Research University-Sorbonne Université, F-75005 Paris, France*

(Dated: April 12, 2022)

Many homogeneously disordered superconducting films follow a Finkelstein mechanism : when disorder combined to electron-electron interactions increase, there is a global decrease of the superconducting energy gap Δ concomitant with the one of the critical temperature. Simultaneously, in most films an emergent granularity develops with increasing disorder and results in the formation of inhomogeneous superconducting puddles. By studying the local electronic properties of a NbN film with scanning tunneling spectroscopy (STS) we show that the inhomogeneous spatial distribution of Δ is locally strongly correlated to a large depletion in the local density of states, associated to a zero-bias anomaly (ZBA). By modelling quantitatively the measured ZBA variations, we show that they correspond to local variations of the film resistivity. This local change in resistivity leads to a local variation of Δ through a local Finkelstein mechanism, furnishing a scenario explaining quantitatively the emerged superconducting inhomogeneities.

Non-magnetic disorder was initially thought to have little effect on the superconducting properties of conventional thin films, as far as time-reversal symmetry is preserved [1, 2]. Decades of intense experimental and theoretical works have ended to the opposite conclusion showing that beyond a critical disorder all systems transit either to a metallic or to an insulating state [3–5]. For thin films that are not single-crystals [6] but consist in coupled nanocrystals two different classes of systems exist. A qualitatively different superconducting behavior is observed between so-called *granular* and *homogeneous* disordered thin films. In *granular* ones a poor electrical coupling between the nanocrystals makes the film a disordered array of Josephson junctions [5, 7–10]. Their superconducting properties are controlled by weak Josephson couplings between phases of local superconducting order parameters of individual nanocrystals. In *homogeneous* ones the nanocrystals are much better electrically coupled to each other. Their superconducting properties are controlled by the subtle interplay between the non-magnetic disorder distribution and electron-electron interactions [3, 4, 11–13].

In *granular* thin films the macroscopic critical temperature T_c is suppressed when disorder grows and intergrain coupling decreases, while the superconducting energy gap Δ almost does not change [5, 7–10]. In contrast, in *homogeneously disordered* films macroscopic measurements show that T_c and Δ monotonously decrease with rising disorder corresponding to $k_F l$ decreasing from a value much larger than one toward unity [3, 4, 11–13] (k_F being

the Fermi wavevector and l the elastic electron mean-free path). This effect has been satisfactorily explained by a reduction of the electronic screening upon increasing disorder and is called the “fermionic” mechanism [14, 15]. Many films like for example, Bi, Pb, MoGe, NbSi behave this way and follow the so-called Finkelstein scenario down to the almost complete destruction of superconductivity [11, 12, 16–18]. Other non-granular thin films like amorphous InO_x or (strongly disordered) TiN show different experimental signatures [19]: when disorder increases the single-particle gap probed by tunneling decouples from the T_c and a pseudogap emerges in a significant temperature range above T_c [20–22]. These latter features are believed to correspond to the so-called “bosonic” scenario, where disorder localizes single-electron wavefunctions and provoke an “emergent granularity” in the superconductor. This weakens and eventually destroys the long-range phase coherence between neighboring superconducting islands [4, 23, 24].

However reality is richer than these two limiting scenarios because most films present an interplay between “fermionic” and “bosonic” effects. In the literature there is a trend to consider that for weak to moderate disorder fermionic effects dominate, while bosonic ones take over for stronger disorder. This kind of combined behavior was seen in TiN [20]. Nevertheless there is a lack of experimental data combining macroscopic and local measurements on the same system to explore carefully this interplay.

In this respect, we focus on NbN thin films. With

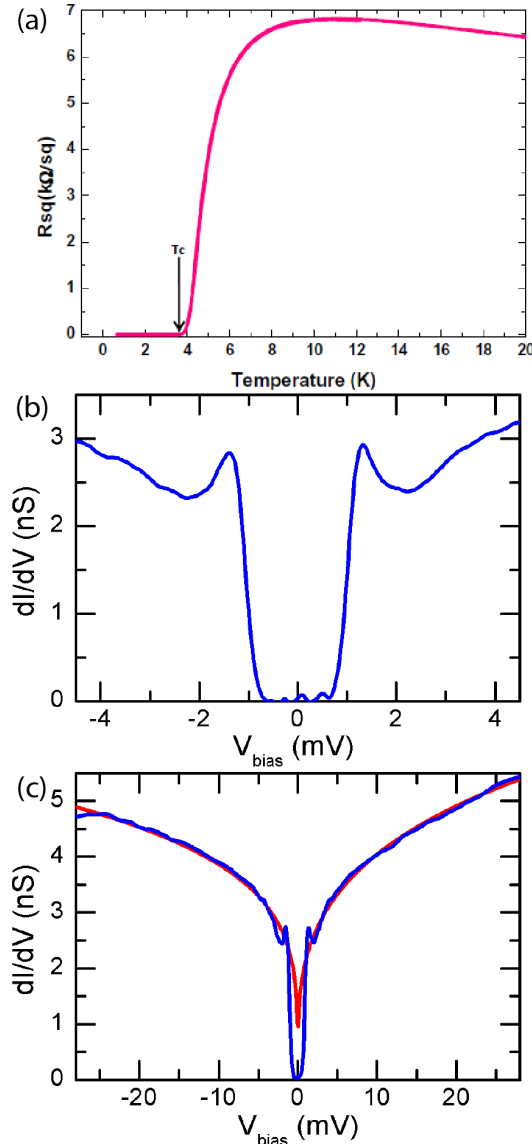


FIG. 1: (a) Square resistance of a 2.1 nm thick NbN film, measured in the same stage where STM is performed. T_c is defined when R_{\square} reaches zero, leading to $T_c = 3.8 \text{ K}$. (b) Typical local $dI/dV(V)$ spectrum measured at $T = 300 \text{ mK}$. Set-point for spectroscopy $V = -10 \text{ mV}$, $I = 150 \text{ pA}$. (c) Local $dI/dV(V)$ spectrum measured at the same location and temperature as in (b) but on a larger voltage scale. The large depletion of the LDOS seen around E_F has a characteristic V-shape due to electron-electron interaction effects enhanced by disorder. The red (lighter) curve shows a power-law fit of this V-shape dependence.

increasing disorder a continuous reduction of Δ and T_c occurs, following the Finkelstein picture, accompanied by emerging and increasing gap inhomogeneities as $k_F l$ decreases [25–27]. The development of these inhomogeneities together with the emergence of a pseudogap regime above T_c were thought to be a signature of “bosonic” effects being established at stronger disorder

in this material [26, 27] (experimentally it is well-developed for $T_c \leq 0.4 T_c^{\text{bulk}}$ and $k_F l \leq 3$), as well as in TiN thin films [20]. In this work we show that in NbN the emergent gap inhomogeneities can be explained by the Finkelstein mechanism: local variations of resistance lead to variations of local energy gap values. To support this claim we provide a direct spatial cross-correlation between local superconducting gap maps and the mapping of the Altshuler-Aronov suppression of the local density-of-states (LDOS).

Our samples consist of ultrathin NbN films grown ex situ on sapphire, structured in nano-crystals of lateral size 2–5 nm [29]. We selected films having a $T_c \approx 0.25 T_c^{\text{bulk}} = 3.8 \text{ K}$, so that seeming “bosonic” properties like gap inhomogeneities and pseudogap features have already developed. The nominal film thickness is about 2.1 nm. We studied their local superconducting properties by scanning tunneling microscopy/spectroscopy (STM/STS) at 300 mK, using PtIr tips, in an ultrahigh vacuum homemade set-up. The presented dI/dV measurements were obtained by numerical derivation of single $I(V)$ curves. T_c was extracted from *in situ* 4-points electrical resistivity measurements performed in the STM stage during the same run as the STM/STS measurements. The temperature dependence of the resistivity before the superconducting transition is shown in Fig. 1a.

STM topography measurements show that the film surface is very flat (see Fig. 2a). The size of the observed nanoscale structures correlate well with the size of the nanocrystals. A characteristic dI/dV spectrum measured locally is shown in Fig. 1b. It presents a fully gapped LDOS with well-defined superconducting coherence peaks. For energies larger than the ones of the coherence peaks, a strong background is seen instead of recovering a standard normal DOS, as in the Bardeen-Cooper-Schrieffer (BCS) case. Fig. 1c enables characterizing this background: it presents a dI/dV spectrum measured on the same location but over a wider energy range about 20 times larger than Δ . We see that the tunneling LDOS is strongly reduced over an energy range much larger than Δ . This zero-bias anomaly (ZBA) is typical of systems where electronic correlations combined to disorder reduce the tunneling DOS at the Fermi level (E_F) [30, 31], an effect first theoretically explained by Altshuler and Aronov.

Fig. 1c shows that for $e|V| \gg \Delta$ the measured LDOS follows a power-law as a function of the applied bias voltage, $dI/dV \propto V^\alpha$. Theoretically such a dependence is expected in the framework of nonperturbative extension [32, 33, 43] of the Altshuler-Aronov theory [30, 31].

The main finding of our work is a systematic spatial correlation between the local energy gap value Δ and the strength of the ZBA, quantified by the exponent α in the power law $dI/dV \propto V^\alpha$. At each square nanometer of the $300 \times 250 \text{ nm}^2$ area shown in Fig. 2a, the local gap value was extracted from the peak-to-peak distance in

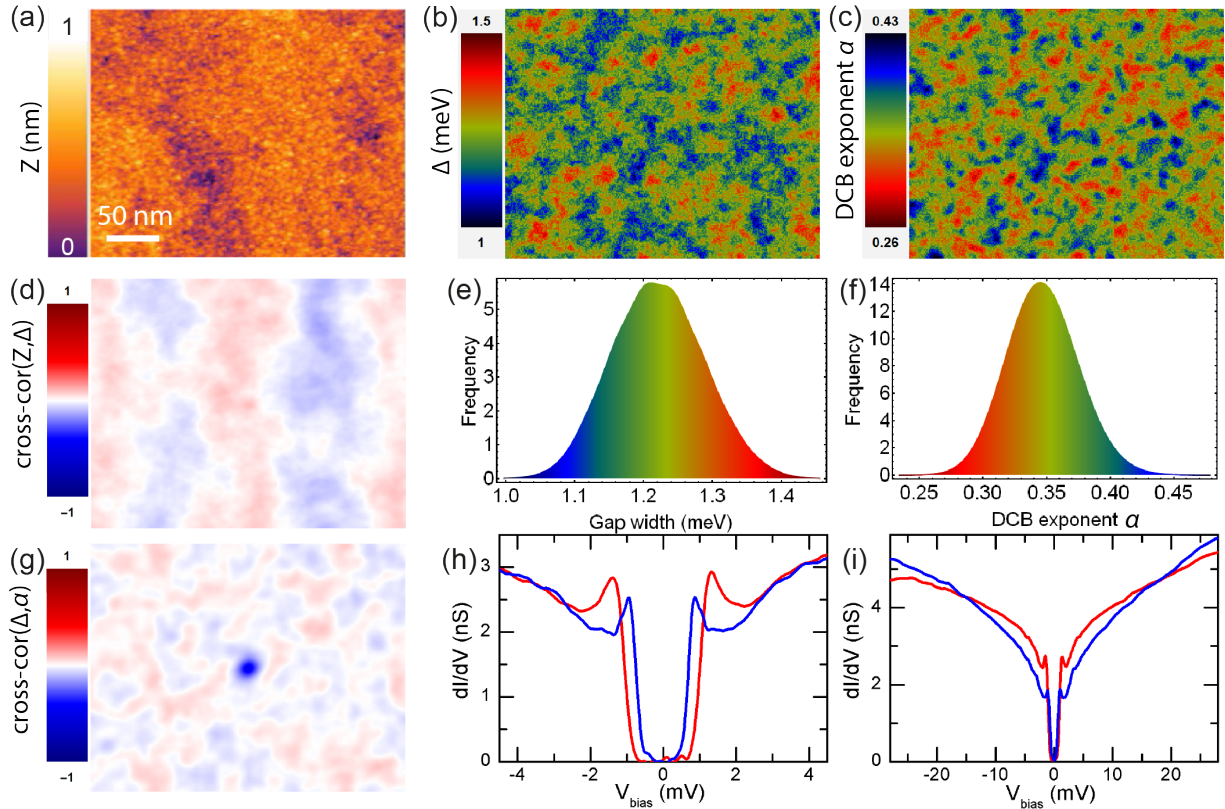


FIG. 2: Spatial cross-correlations between variations of local the superconducting gap Δ and the ZBA exponent α . Measurements done at 300 mK in zero magnetic field. (a) STM topography of a 300×250 nm² area of the NbN sample (height variation Z in nm). (b) Color-coded map showing the local energy gap Δ (in meV) measured in area (a) by STS. (c) Color-coded map showing the local exponent α in area (a). (d) Color-coded map showing the cross-correlation between the topography $Z(x, y)$ shown in (a) and the gap map $\Delta(x, y)$ shown in (b). No cross-correlations are found. (e) Histogram of Δ values occurring in (b). (f) Histogram of α values occurring in (c). (g) Color-coded map showing the cross-correlation between the gap map $\Delta(x, y)$ shown in (b) and the exponent map $\alpha(x, y)$ shown in (c). A strong spatial anti-correlation is found: where local electron-electron interactions are stronger (larger $\alpha(x, y)$) $\Delta(x, y)$ is smaller and vice-versa. (h): Representative dI/dV spectra of the regions seen in (b). Brighter (respectively darker) spectra are measured in brighter (darker) regions of panel (b). (i) Same spectra as in (h) but over an energy scale 20 to 30 times larger than Δ . Brighter (respectively darker) spectra are measured in brighter (darker) regions of panel (c).

each dI/dV curve. The extracted map of the gap values is shown in Fig. 2b. The gap energy ranges between 1 and about 1.5 meV and its spatial distribution shows emerging local inhomogeneities, as reported previously in several similar systems [20, 26–28]. $\Delta = 1.2$ meV is used below for the typical gap value.

We call *supergrain* a region with a nearly constant gap. Its size $l_{\text{sg}} \approx 30$ nm is much larger than the low- T coherence length $\xi(0) \approx 5$ nm. The histogram of the gap values is shown in panel 2e and is close to a Gaussian distribution. We provide now for the first time a local mapping of the disorder distribution combined to electron interaction effects which together are responsible for the spatial distribution of the gap inhomogeneities. At each location the gap value was measured, the local ZBA exponent α was also extracted in the energy range [5;30] mV (the slight asymmetry in our spectra between positive and negative energies probably comes from a non-constant

tip DOS).

The map of the exponent α is presented in panel 2c and its histogram in panel 2f. The correlation length of α is $l_{\text{ZBA}} \approx 15$ nm. The normalized cross-correlation between the gap map and the exponent map is shown in panel 2g. A very large anti-correlation of about -0.5 at coincident points is found. This implies that the larger is the local energy gap value Δ , the smaller is the local ZBA exponent α , as illustrated on panels 2h and i. The dI/dV spectrum with a large Δ has a flatter ZBA background (red curve), and vice versa (blue curve).

One could naively think a direct one-to-one correspondence between the spatial distribution of the NbN nanocrystals encoded in the STM topography and the gap map or ZBA exponent map could exist. In fact we found no cross-correlation between the local gap values and the topography of the probed area (see panel 2d). This is in agreement with our previous work [28]. In contrast,

the present results furnish a new way of characterizing locally and quantitatively the underlying disorder distribution combined to electron interaction effects which lead to the appearance of supergrains of size l_{sg} .

The low-temperature value of the coherence length can be estimated as $\xi(0) = \sqrt{\hbar D/\Delta} \approx 5.2$ nm. It corresponds to the diffusion coefficient $D \approx 0.5$ cm²/s obtained from $dB_{c2}(T)/dT$ data close to T_c , see Ref. [29]. With the mean free path $l \approx 0.5$ nm [29], we find for the elastic scattering time: $\tau = l^2/3D \approx 1.7 \times 10^{-15}$ s.

We present now a quantitative analysis of the data in the framework of the Finkelstein theory modified for the case of inhomogeneous local resistance. According to Refs. [30–32, 43, 44] the tunneling DOS suppression in an interacting diffusive normal metal, $\nu(E)$, is determined by the spreading resistance between the diffusive scale and the field propagation scale (see details in [41]). Relevant eV values (dozens of mV) are much smaller than $\hbar/\tau \approx 0.33$ eV, justifying well the diffusive regime. In the 2D geometry, the log-normal dependence of $\nu(E)$ [43, 44] can be approximated by a power law with the energy-dependent exponent $\alpha(V) = (R_{\square}/2\pi R_Q) \ln(\hbar\omega_0/eV)$, where $R_Q = \hbar/e^2 = 25.8$ kΩ is the resistance quantum and ω_0 is the plasma frequency. Taking $\hbar\omega_0 \approx 10$ eV from Ref. [29], $V = 10$ mV (typical voltage scale for experimental determination of α , see Fig. 1c) and $R_{\square} = 6.8$ kΩ (maximal sheet resistance R_{\square}^{max} before the transition, see Fig. 1a), we obtain $\alpha = 0.29$. This value is quite close to the mean value 0.35 measured experimentally. The small discrepancy could be related to the use of an underestimated R_{\square}^{max} that is significantly affected by superconducting fluctuations, whereas the ZBA involves larger frequencies, where this suppression is less efficient. We conclude that the mean value of the ZBA exponent $\langle \alpha(\mathbf{r}) \rangle$ is well described by the theory developed in Refs. [43, 44].

The key point in our explanation of inhomogeneity seen in $\alpha(\mathbf{r})$ and $\Delta(\mathbf{r})$ is an assumption that both of them originate from fluctuations in the local 2D resistivity $\rho(\mathbf{r}) = R_{\square} + \delta\rho(\mathbf{r})$. Using the concept of spreading resistance to calculate $\delta\alpha(\mathbf{r}, V)$, we obtain (see [41]):

$$\delta\alpha(\mathbf{r}, V) = \frac{\delta\rho(\mathbf{r})}{2\pi R_Q} \ln \frac{eV}{\hbar D/l_{\text{ZBA}}^2}. \quad (1)$$

Using the experimentally measured dispersion of the ZBA exponent $\sigma_{\alpha} = 0.028$ (see panel 2f), its correlation length $l_{\text{ZBA}} \approx 15$ nm and taking $V = 10$ mV, we find $eV/(\hbar D/l_{\text{ZBA}}^2) \approx 70$ and hence obtain the sheet resistance dispersion $\sigma_{\rho} = 1.1$ kΩ, which is 16 % of R_{\square}^{max} .

Suppression of the superconducting order parameter in regions with larger local resistivity is explained by the Finkelstein mechanism. In general, one should distinguish between fluctuations coming from small ($q < q_D$) and large ($q > q_D$) momenta, where $q_D = \sqrt{\omega_D/D}$ with ω_D the Debye frequency. For our NbN film we estimate $\hbar\omega_D \approx 300$ K, $q_D \approx 1$ nm⁻¹. The low-momentum con-

tribution is given by the usual log-cube 2D expression

$$\frac{\delta\Delta(\mathbf{r})}{\langle \Delta \rangle} \approx -\frac{\delta\rho(\mathbf{r})}{6\pi R_Q} \ln^3 \frac{\hbar\omega_D}{\Delta(0)}, \quad (2)$$

cut off at the Debye frequency [41]. The high-momentum contribution can be expressed in terms of the renormalization of the BCS coupling constant $\lambda(\mathbf{r})$. Substituting the resistivity dispersion $\sigma_{\rho} = 1.1$ kΩ into Eq. (2), we obtain for the relative gap dispersion $\sigma_{\Delta}/\langle \Delta \rangle = 0.074$, whereas the experimental value is 0.057 (see panel 2e). Note that Eq. (2) contains a large degree of uncertainty: the precise value of $\hbar\omega_D$ being unknown, σ_{Δ} can only be determined with roughly 50 % accuracy. Nevertheless, the fact that Eq. (2) nearly describes the measured gap dispersion indicates that the high-momentum contribution to fluctuations of $\Delta(\mathbf{r})$ is absent. This behavior could be modeled by a fluctuation of the 2D resistivity due to interface resistance variations between neighboring crystallites, while the 3D resistivity within each crystallite remains identical.

We have shown that local probe spectroscopic studies are able to demonstrate a direct relation between properties of the electronic excitation spectrum pertinent to the lowest-energy scale: the superconducting gap (~ 1 meV) on one hand, and to much higher (few dozens of meV) energy scales relevant to the soft Coulomb anomaly. This supports the relevance of “fermionic mechanism” and Finkelstein theory for superconductivity suppression by disorder. However we point out that for our ultrathin film the ratio $\Delta(0)/k_B T_c \approx 3.7$ is twice larger than the BCS theory prediction 1.76, and significantly larger than the value of 2.1 known for thick NbN films [29]. It could be partly due to thermal fluctuations which suppress T_c with respect to its mean-field value $T_c^{(0)}$. However the whole effect appears too strong and an additional contribution to the total spectral gap likely comes from a developing “pseudo-gap” effect [22].

In conclusion, we demonstrate sharp spatial anti-correlations in highly resistive NbN thin films between the local magnitude of the superconducting energy gap Δ and the value of the Coulomb zero-bias anomaly exponent α . Our results are in agreement with predictions of the Finkelstein theory for “fermionic mechanism” of superconductivity suppression by disorder. This is generally expected for superconducting materials when: (a) a strong Coulomb interaction exists between conduction electrons, and (b) the spatial scale characteristic of the inhomogeneities of the Coulomb zero-bias anomaly much exceeds the superconducting coherence length.

We thank D. S. Antonenko for useful discussions. This work was supported by the French ANR project SUPER-STRIPES under the reference number ANR-15-CE30-0026, by Skoltech NGP Program (Skoltech-MIT joint project) and by the Russian Academy of Sciences Program “Low temperature physics”.

* Electronic address: christophe.brun@sorbonne-universite.fr

[1] A. A. Abrikosov and L. P. Gorkov, On the theory of superconducting alloys: 1. The electrodynamics of alloys at absolute zero. *JETP* **8**, 1090 (1958).

[2] Anderson, P. W. Theory of dirty superconductors. *J. Phys. Chem. Solids* **11**, 26 (1959).

[3] A. M. Goldman and N. Marković, Physics today November, 39 (1998).

[4] M. V. Feigel'man, L. B. Ioffe, V. E. Kravtsov, and E. Cuevas, Fractal superconductivity near localization threshold. *Ann. Phys.* **325** 1390 (2010).

[5] V. F. Gantmakher and V. T. Dolgopolov, Physics - Uspekhi **53**, 1-49 (2010).

[6] C. Brun, T. Cren and D. Roditchev, Supercond. Sci. Technol. **30**, 013003 (2017).

[7] K. B. Efetov, Phase transition in granulated superconductors. *Sov. Phys. JETP* **51**, 1015 (1980).

[8] B. G. Orr, H. M. Jaeger, and A. M. Goldman, Local superconductivity in ultrathin Sn films. *Phys. Rev. B* **32**, 7586 (1985).

[9] White, A.E., Dynes, R.C. and Gorno, J.P. Destruction of superconductivity in quench-condensed two-dimensional films. *Phys. Rev. B* **33**, 3549 (1986).

[10] Jaeger, H.M. *et al.*. Threshold for superconductivity in ultrathin amorphous gallium films. *Phys. Rev. B* **34**, 4920 (1986).

[11] J. M. Graybeal, and M. R. Beasley, *Phys. Rev.* **29**, 4167 (1984).

[12] R. C. Dynes, A. E. White, J. M. Graybeal, and J. P. Gorno, *Phys. Rev. Lett.* **57**, 2195 (1986).

[13] Haviland, D.B. *et al.* Onset of superconductivity in the two-dimensional limit. *Phys. Rev. Lett.* **62**, 2180 (1989).

[14] A.M. Finkel'stein, Pis'ma ZhETF **45**, 37 (1987) [JETP Letters **45**, 46 (1987)].

[15] A.M. Finkel'stein, *Physica B* **197**, 636 (1994).

[16] J. M. Valles, Jr., R. C. Dynes, and J. P. Gorno, *Phys. Rev. Lett.* **69**, 3567 (1992).

[17] O. Crauste *et al.*, *J. Phys.: Conf. Series* **150**, 042019 (2009).

[18] O. Crauste *et al.*, *Phys. Rev. B* **87**, 144514 (2013).

[19] D. Shahar, and Z. Ovadyahu, *Phys. Rev. B* **46**, 10917 (1992).

[20] B. Sacépé *et al.*, *Phys. Rev. Lett.* **101**, 157006 (2008).

[21] B. Sacépé *et al.*, *Nat. Comm.* **1**, DOI: 10.1038/ncomms1140 (2010).

[22] B. Sacépé *et al.*, *Nat. Phys.* **7**, 239 (2011).

[23] A. Ghosal, M. Randeria, and N. Trivedi, *Phys. Rev. Lett.* **81**, 3940 (1998); A. Ghosal, M. Randeria, and N. Trivedi, *Phys. Rev. B* **65**, 014501 (2001).

[24] K. Bouadim, Y. L. Loh, M. Randeria, and N. Trivedi, *Nature Phys.* **7**, 884 (2011).

[25] S. P. Chockalingam *et al.* *Phys. Rev. B* **79**, 094509 (2009); M. Mondal *et al.* *Phys. Rev. Lett.* **106**, 047001 (2011).

[26] Y. Noat *et al.* *Phys. Rev. B* **88**, 014503 (2013).

[27] A. Kamlapure *et al.* *Sci. Rep.* **3**, 2979; DOI:10.1038/srep02979 (2013).

[28] C. Carbilliet *et al.* *Phys. Rev. B* **93**, 144509 (2016).

[29] A. Semenov *et al.* *Phys. Rev. B* **80**, 054510 (2009).

[30] B. L. Altshuler, A. G. Aronov, and P. A. Lee, *Phys. Rev. Lett.* **44**, 1288 (1980).

[31] B. L. Altshuler and A. G. Aronov, in *Electron-Electron Interactions in Disordered Systems*, edited by A. L. Efros and M. Pollak (North Holland, 1985).

[32] G.-L. Ingold and Yu. V. Nazarov, in *Single Charge Tunneling*, edited by H. Grabert and M. Devoret, NATO ASI, Ser. B Vol. 294 (Plenum, New York, 1992), p. 21.

[33] J. Rollbühler and H. Grabert, *Phys. Rev. Lett.* **87**, 126804 (2001).

[34] C. Brun *et al.*, *Phys. Rev. Lett.* **108**, 126802 (2012).

[35] L. Serrier-Garcia *et al.*, *Phys. Rev. Lett.* **110**, 157003 (2013).

[36] D. Roditchev *et al.*, *Nat. Phys.* **11**, 332 (2015).

[37] Y. Dubi, Y. Meir, and Y. Avishai, *Nature* **449**, 876 (2007).

[38] M. Mondal *et al.*, *Phys. Rev. Lett.* **107**, 217003 (2011).

[39] G. Seibold, L. Benfatto, C. Castellani, and J. Lorenzana, *Phys. Rev. Lett.* **108**, 207004 (2012).

[40] L. P. Gor'kov and E. I. Rashba, Superconducting 2D System with Lifted Spin Degeneracy: Mixed Singlet-Triplet State. *Phys. Rev. Lett.* **87**, 037004 (2001).

[41] Supplemental Material.

[42] A. I. Larkin and Yu. N. Ovchinnikov, *Zh. Eksp. Teor. Fiz.* **61**, 2147 (1971) [Sov. Phys. JETP **34**, 1144 (1972)].

[43] L. S. Levitov and A. V. Shytov, *Pis'ma Zh. Eksp. Teor. Fiz.* **66**, 200 (1997) [JETP Lett. **66**, 214(1997)].

[44] A. Kamenev and A. V. Andreev, *Phys. Rev. B* **60**, 2218 (1999)